

# Shift-Invariant Multichannel Blind Restoration

Filip Šroubek, Jan Flusser  
Institute of Information Theory and Automation  
Academy of Sciences of the Czech Republic  
Pod vodárenskou věží 4, 182 08, Praha 8  
{sroubekf, flusser}@utia.cas.cz

## Abstract

*Existing multichannel blind restoration techniques are prone to noise, assume perfect spatial alignment of channels and a correct estimation of blur size. We develop an alternating minimization scheme based on maximum a posteriori probability estimation with a priori distribution of blurs derived from the multichannel framework and a priori distribution of original images defined by the total variation semi-norm. This stochastic approach enables us to recover the blurs and the original image from channels severely corrupted by noise. We observe that the exact knowledge of the blur size is not necessary and we show that translation misregistration up to a certain extent can be automatically removed in the restoration process.*

## 1. Introduction

In many applications such as microscopy imaging, remote sensing, and astronomical imaging, observed images are degraded by unknown or partially known distortion. Examples of most common distortions are atmospheric turbulence, relative motion between a camera and an object or an out-of-focus camera. Restoration of the degraded images is generally necessary before any further image processing or segmentation can take place. We talk about *multichannel blind restoration*, when several blurred versions of one scene are obtained through different acquisition channels and the task is to recover the original image from the blurred images solely without any knowledge of the channel properties. Examples of such multichannel (MC) measurements are common, e.g., in remote sensing and astronomy, where the same scene is observed at different times through the time-varying inhomogeneous atmosphere; in confocal microscopy, where images of the same sample are acquired at different focus depth; or in broadband imaging through a physically stable medium but which has a different transfer function at different frequencies.

Intuitively, one may expect that the blind restoration problem is greatly simplified by the availability of different channels. In the noise-free environment, channel blurs can be precisely recovered if a mild assumption of channel coprimeness is satisfied, i.e. a sufficient diversity of channel blurs is assured. Harikumar et al. [5, 4] and independently Giannakis et al.[3] proposed two solutions to the MC problem: direct estimation of blurs from degraded images and construction of restoration FIR filters from degraded images. Both approaches are vulnerable to noise corruption and may brake down even at moderate noise levels. Using a special matrix constructed by the degraded images, Pai et al. [6, 7] proposed a multichannel restoration algorithm, that directly recovers the original image from the null space or from the range of the matrix. In the noisy case, this algorithm performs better than Harikumar's approach.

The mentioned algorithms lack robustness, assume correct size of blurs and perfect spatial alignment (*registration*) of channels. These assumptions are seldom true in real applications and have not yet been considered in previous works dedicated to multichannel restoration.

In this paper, we address the issues of robustness, blur size, and misalignment. An alternating minimization (AM) algorithm as a solution to a maximum a posteriori (MAP) estimator is given here. The estimator is based on the total variation integral in the MC setting. We examine the minimization algorithm for its ability to alleviate the blur-oversized problem and show that the channel misalignment can be perfectly neutralized by properly oversizing the blur support.

## 2 Problem formulation

We first define the single-input multiple-output degradation model in the discrete domain  $\mathbb{N}^2$  as follows. Each image function has a finite rectangular support and can be expressed as a column vector by concatenating its columns. In this manner, let the vector  $\mathbf{u}$  denote the original (input) image of size  $S_u \in \mathbb{N}^2$ . The input image propagates

through  $K$  different channels that behave as linear filters (matrices  $\mathbf{H}_k$ ) with finite impulse responses (masks)  $\mathbf{h}_k$ ,  $k \in \{1, \dots, K\}$ . Let the maximum support size of the masks be  $S_h \in \mathbb{N}^2$ . In each channel, the image is further degraded with additive white Gaussian noise (AWGN)  $\mathbf{n}_k$  of variance  $\sigma^2$  and shifted by  $t_k \in \mathbb{N}^2$ , where  $S_t \in \mathbb{N}^2$  denotes the maximum observed shift. On the output, we receive degraded and shifted images  $\mathbf{z}_k$ . Using the above vector-matrix notation, the whole degradation model can be then expressed as

$$\mathbf{z}_k = \mathbf{T}_k \mathbf{H}_k \mathbf{u} + \mathbf{n}_k, k = 1, \dots, K,$$

where  $\mathbf{T}_k$  is a translation operator shifting an image by  $t_k$  pixels, i.e. a linear filter with the  $\delta$ -function at the position  $t_k$ . It is easy to verify that the matrix product  $\mathbf{T}_k \mathbf{H}_k = \mathbf{G}_k$  defines convolution with a mask  $\mathbf{g}_k$  that is a shifted version of the mask  $\mathbf{h}_k$  with the maximum support size  $S_g = S_h + S_t$ . By concatenating the channels, the previous equation can be rewritten in two equivalent forms

$$\mathbf{z} = \mathbf{G}\mathbf{u} + \mathbf{n} = \mathbf{U}\mathbf{g} + \mathbf{n}, \quad (1)$$

where  $\mathbf{z} \equiv [\mathbf{z}_1^T, \dots, \mathbf{z}_K^T]^T$ ,  $\mathbf{G} \equiv [\mathbf{G}_1^T, \dots, \mathbf{G}_K^T]^T$ ,  $\mathbf{n} \equiv [\mathbf{n}_1^T, \dots, \mathbf{n}_K^T]^T$ ,  $\mathbf{g} \equiv [\mathbf{g}_1^T, \dots, \mathbf{g}_K^T]^T$ , and  $\mathbf{U}$  is a block-diagonal matrix with  $K$  blocks each performing convolution with the image  $\mathbf{u}$ .

Adopting a stochastic approach, the problem of image restoration can be formulated as an MAP estimation. We assume that the images  $\mathbf{u}$ ,  $\mathbf{g}$  and  $\mathbf{z}$  are random vector fields with given probability density functions (pdf)  $p(\mathbf{u})$ ,  $p(\mathbf{g})$  and  $p(\mathbf{z})$ , respectively, and we look for such realizations of  $\mathbf{u}$  and  $\mathbf{g}$  which maximize the a posteriori probability  $p(\mathbf{u}, \mathbf{g}|\mathbf{z})$ . According to the Bayes rule, the relation between a priori probabilities  $p(\mathbf{u})$ ,  $p(\mathbf{g})$  and the a posteriori probability is  $p(\mathbf{u}, \mathbf{g}|\mathbf{z}) \propto p(\mathbf{z}|\mathbf{u}, \mathbf{g})p(\mathbf{u})p(\mathbf{g})$ . The conditional pdf  $p(\mathbf{z}|\mathbf{u}, \mathbf{g})$  follows from (1) and from our assumption of AWGN, i.e.,

$$p(\mathbf{z}|\mathbf{u}, \mathbf{g}) \propto \exp \left\{ -\frac{1}{2\sigma^2} (\mathbf{z} - \mathbf{G}\mathbf{u})^T (\mathbf{z} - \mathbf{G}\mathbf{u}) \right\}. \quad (2)$$

A space of bounded variation (BV) functions is widely accepted as a proper setting for real images. This has been proved many times by demonstrating very good anisotropic denoising properties of the total variation semi-norm  $TV(u) = \int |\nabla u(x)| dx$  that is well defined only in the BV space. Since the variational integral is highly nonlinear and not continuous at  $\nabla u(x) = 0$ , a special attention must be paid to its discretization and several relaxed linearization schemes were proposed. Following the half-quadratic regularization scheme in [1] that introduces an auxiliary variable, we can express the a priori distribution of the original image as

$$p(\mathbf{u}, v) \propto \exp \left\{ -\frac{1}{2} \mathbf{u}^T \mathbf{L}(v) \mathbf{u} \right\}, \quad (3)$$

where  $v$  is the auxiliary variable similar to Geman's line process [2] and which is defined as

$$v(x) = \begin{cases} 1/|\nabla u(x)| & \text{if } |\nabla u(x)| > \epsilon \\ 1/\epsilon & \text{otherwise,} \end{cases}$$

where  $\epsilon$  is a relaxation parameter. Matrix  $\mathbf{L}(v)$  is a block tridiagonal matrix constructed by  $v$  that performs shift-variant convolution with  $v$ . In relatively flat regions,  $|\nabla u(x)| \leq \epsilon$ ,  $\mathbf{L}(v)$  becomes the Laplacian operator. In regions with high image gradient,  $|\nabla u(x)| > \epsilon$ ,  $\mathbf{u}^T \mathbf{L}(v) \mathbf{u}$  calculates the TV semi-norm of the image  $\mathbf{u}$ .

The prior distribution  $p(\mathbf{g})$  can be derived from the fundamental multichannel constrain stated by Harikumar [5, 4] and Giannakis [3]. Let  $\mathbf{Z}_k$  denote the convolution matrix with the degraded image  $\mathbf{z}_k$ . If noise  $\mathbf{n}_k$  is zero and the original channel masks  $\{\mathbf{h}_k\}$  are "weakly coprime", i.e. their only common factor is a scalar constant, then

$$\mathbf{Z}_i \mathbf{g}_j - \mathbf{Z}_j \mathbf{g}_i = \mathbf{0}, \quad 1 \leq i < j \leq K. \quad (4)$$

If both the maximum size of blurs and the shift between the channels,  $S_g$ , are known, the solution is  $\{\alpha \mathbf{g}_k\}$  for any scalar  $\alpha$ . If  $S_g$  is not known, it must be first estimated and two distinct situations arise. If  $S_g$  is underestimated, zero vector is the only solution of (4). If  $S_g$  is overestimated, then the space of all solutions of (4) contains the correct masks  $\{\mathbf{g}_k\}$  and the dimensionality of this solution space is proportional to the degree of the overestimation. The system of equations in (4) can be expressed as one equation

$$\mathbf{Z}\mathbf{g} = \mathbf{0}, \quad (5)$$

where

$$\mathbf{Z} \equiv \begin{pmatrix} \mathbf{Z}_1^T & \dots & \mathbf{Z}_{K-1}^T \\ \mathbf{0} & \dots & \mathbf{0} & \mathbf{Z}_{i+1} & \dots & -\mathbf{Z}_i & \dots \\ \vdots & \ddots & \vdots & \vdots & \ddots & \vdots & \vdots \\ \mathbf{0} & \dots & \mathbf{0} & \mathbf{Z}_K & \dots & \dots & -\mathbf{Z}_i \end{pmatrix}$$

$\underbrace{\hspace{10em}}_{i-1 \text{ blocks}} \quad \underbrace{\hspace{10em}}_{K-i+1 \text{ blocks}}$

for  $i = 1, \dots, K-1$ . If the AWGN noise term  $\mathbf{n}_p$  is present, it follows from (1) that the left-hand side of (5) is not zero but equals to a realization of a Gaussian process with zero mean and covariance  $\mathcal{C}$  given by

$$\mathcal{C} = \sigma^2 \mathcal{G}\mathcal{G}^T, \quad (6)$$

where

$$\mathcal{G} \equiv \begin{pmatrix} \mathcal{G}_1^T & \dots & \mathcal{G}_{K-1}^T \\ \mathbf{0} & \dots & \mathbf{0} & \mathcal{G}_{i+1} & \dots & -\mathcal{G}_i & \dots \\ \vdots & \ddots & \vdots & \vdots & \ddots & \vdots & \vdots \\ \mathbf{0} & \dots & \mathbf{0} & \mathcal{G}_K & \dots & \dots & -\mathcal{G}_i \end{pmatrix}$$

$\underbrace{\hspace{10em}}_{i-1 \text{ blocks}} \quad \underbrace{\hspace{10em}}_{K-i+1 \text{ blocks}}$

for  $i = 1, \dots, K - 1$ . Finally, the prior pdf  $p(\mathbf{g})$  is given by

$$p(\mathbf{g}) \propto \exp\left\{-\frac{1}{2}\mathbf{g}^T \mathbf{Z}^T \mathbf{C}^{-1} \mathbf{Z} \mathbf{g}\right\}. \quad (7)$$

Our numerical experiments have shown that the covariance matrix  $\mathbf{C}$  can be approximated by a constant diagonal matrix  $(2\sigma^2/K)\|\mathbf{g}\|^2\mathbf{I} = (2\sigma^2/K)\|\mathbf{h}\|^2\mathbf{I}$ , which greatly simplifies the calculation and does not inflict the restoration. Here  $\|\cdot\|$  denotes the  $l_2$  norm.

Combining (2), (3) and (7), we get

$$p(\mathbf{u}, \mathbf{g}|\mathbf{z}) \propto \exp\left\{-\frac{1}{2}\left(\frac{1}{\sigma^2}(\mathbf{z} - \mathbf{G}\mathbf{u})^T(\mathbf{z} - \mathbf{G}\mathbf{u}) + \mathbf{u}^T \mathbf{L}(v)\mathbf{u} + \mathbf{g}^T \mathbf{Z}^T \mathbf{C}^{-1} \mathbf{Z} \mathbf{g}\right)\right\}$$

and the MAP estimation is equivalent to minimizing an energy functional

$$E(\mathbf{u}, \mathbf{g}) = \frac{1}{\sigma^2}(\mathbf{z} - \mathbf{G}\mathbf{u})^T(\mathbf{z} - \mathbf{G}\mathbf{u}) + \mathbf{u}^T \mathbf{L}(v)\mathbf{u} + \mathbf{g}^T \mathbf{Z}^T \mathbf{C}^{-1} \mathbf{Z} \mathbf{g}. \quad (8)$$

Such problems can be solved by means of genetic algorithms, e.g., simulated annealing. However, we have adopted a simple approach of alternating minimizations of  $E$  over  $\mathbf{u}$  and  $\mathbf{g}$  which, in case of constant  $\mathbf{C}$ , leads to two linear equations:

$$\begin{aligned} (\mathbf{U}^T \mathbf{U} + \sigma^2 \mathbf{Z}^T \mathbf{C}^{-1} \mathbf{Z})\mathbf{g} &= \mathbf{U}^T \mathbf{z} \\ (\mathbf{G}^T \mathbf{G} + \sigma^2 \mathbf{L}(v))\mathbf{u} &= \mathbf{G}^T \mathbf{z} \end{aligned} \quad (9)$$

Each minimization step is a solution to a simple convex problem (but not necessarily strictly convex, especially, when  $g$  is oversized). The conjugate gradient (CG) method is used to solve the second equation in (9) because the matrices are extremely large and direct solution methods cannot be applied here.  $E$  as a function of both variables  $\mathbf{u}$  and  $\mathbf{g}$  is, however, not convex. Therefore, we cannot guarantee, in general, that the global minimum is reached by the AM-MAP algorithm. Nevertheless, our experiments have shown good convergence properties when the correct mask size was used. We also assume that the noise variance  $\sigma^2$  is known. If this is not the case, the noise variance can be assessed by standard noise estimation methods or an approach of ‘‘trial and error’’ can be considered. The impact of wrong  $\sigma^2$  can be easily observed. If the parameter is too small, i.e. we assume less noise, the restoration process begins to amplify noise in the image. If the parameter is too big, the restoration process starts to segment the image.

### 3 Shift-invariant restoration

To assess the quality of restoration, we use the percentage mean square error of the estimated image  $\hat{\mathbf{u}}$  with respect

to the original image  $\mathbf{u}$  defined as

$$\text{PMSE}(\mathbf{u}) \equiv 100 \frac{\|\hat{\mathbf{u}} - \mathbf{u}\|}{\|\mathbf{u}\|}.$$

The first experiment demonstrates the capability of the AM-MAP algorithm to recover the original image from two degraded and shifted versions thereof, when the maximum shift between any two channels is known. The standard  $128 \times 128$  ‘‘Lena’’ image is degraded with two  $5 \times 5$  blurs. One blurred image is shifted by  $10 \times 20$  pixels and then both images are cropped to the same size; see Fig. 1. The AM algorithm is initialized with the correctly estimated blur size  $15 \times 25$ . The restored image and blurs are shown in Fig. 2. The blurs are perfectly recovered and properly shifted. The restored image matches the original one, showing only minor artifacts close to the borders where only data from one channel were available. The same experiment is conducted again but Gaussian noise SNR = 30 dB is added to the blurred and shifted input images in Fig. 1. (Recall that SNR decreases as noise variance increases.) Obtained results in Fig. 3 illustrate satisfying restoration.

We also compare the performance of Pai’s method [7] with our algorithm for different levels of noise. The Pai approach directly recovers the original image by calculating the maximum singular vector of a special matrix. The *QR decomposition* is necessary for the construction of this matrix and the *power method* (or any other iterative method for eigenvector computation) is used to find the maximum singular vector, i.e the original image. Although the Pai method is not iterative in its definition, it requires numerical iterative methods and thus approaches the complexity of our inherently iterative algorithm. We use four randomly generated  $3 \times 3$  blurs to obtain four blurred ‘‘Lena’’ images. The images are then mutually translated so that centers of the images are in corners of a  $5 \times 5$  square. Noise is added with SNR = 10, 20, 30, 40 and 50 dB, respectively. The maximum shift and the size of blurs are assumed to be known and therefore both methods are initialized with the correct blur size  $8 \times 8$ . For each SNR, the experiment is repeated with different blurs 10 times and stopped after 50 iterations in the AM-MAP case. The mean PMSE and standard deviation is calculated over these 10 estimated images and plotted in Fig. 4. Clearly, the AM-MAP performs better than the Pai method for every SNR.

In the next experiment, we evaluate the performance of the AM-MAP algorithm with respect to the channel misalignment. Degraded images are prepared in similar fashion as in the previous experiment but this time the maximum translation between any two channels varies from 0 to  $5 \times 5$  pixels to simulate inaccurate registration. For each shift, the algorithm is repeated 10 times with different blurs and is every time initialized with the blur size  $8 \times 8$ . The calculated mean PMSE and standard deviation is given in Figs. 5



**Figure 1. The “Lena” image degraded with two  $5 \times 5$  blurs (bottom). Mutual translation between the images is  $10 \times 20$  pixels.**

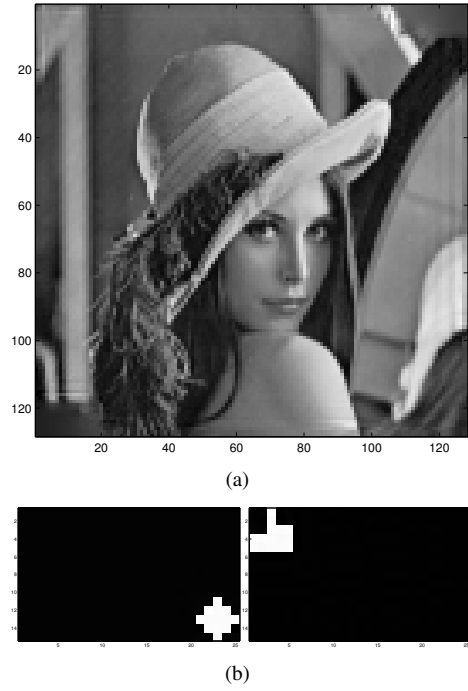


**Figure 2. Perfect noise-free AM-MAP restoration: (a) recovered “Lena” image, (b) recovered blurs and  $10 \times 20$  shift between channels**

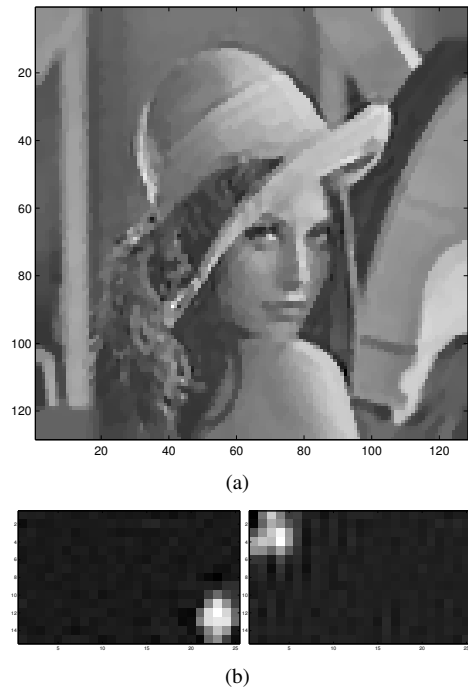


**Figure 3. Noisy AM-MAP restoration (30dB): (a) recovered “Lena” image, (b) recovered blurs and  $10 \times 20$  shift between channels**

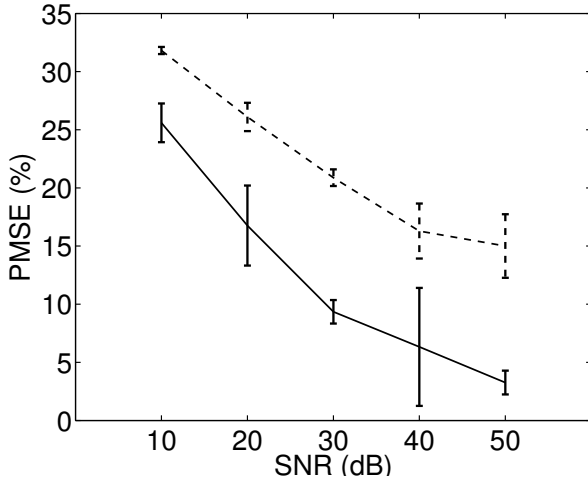


**Figure 4. Comparison of the AM-MAP algorithm (solid) and the Pai method (dashed): Mean PMSE and standard deviation (vertical abscissae) of the restored images over 10 different degradations and for different SNR.**

and 6. For low SNR's around 10 and 20 dB, PMSEs are almost constant, which demonstrates a very good stability of the algorithm with respect to the mask overestimation. In the case of high SNR's, see Fig. 6, we can observe a steady growth of the restoration error as the shift increases and then a dramatic performance gain for shift 5. This sharp error decrease is due to much better convergence of the algorithm if the blur size is correctly estimated, which, in our case, corresponds to shift 5. Results for low SNR's in Fig. 5 do not exhibit such dramatic performance gains as the impact of noise prevails over the blur size overestimation.

Finally, to demonstrate the applicability of the AM-MAP algorithm, we have performed an experiment with real data. This experiment was motivated by many practical situations where we have to handle images degraded by random vibration blur. This problem appears frequently in industrial visual inspection when the camera is mounted on a vibrating machine or when a stationary camera monitors vibrating environment. A text label (a part of a standard newspaper page) was attached to a vibrating machine. The label was monitored under poor light conditions by a standard digital camera mounted on a tripod. The camera exposure time was set at 1/15s which was comparable to the period of irregular vibrations of the machine. Three cropped images of the label acquired with the camera were used as the input channels of AM-MAP; see Fig. 7. Note strong shift blurs due to the machine movement and clear spatial misalignment of the channels. The AM-MAP algorithm was initialized with the blur size  $10 \times 10$ ,  $\sigma^2 = 0.01$

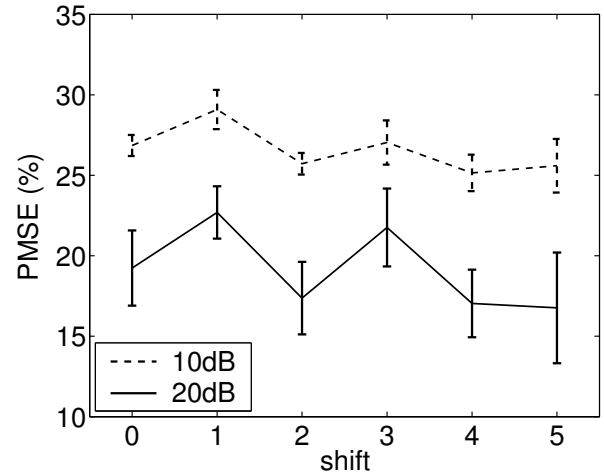


**Figure 5. AM-MAP algorithm performance on misaligned channels: Mean PMSE and standard deviation (vertical abscissae) of restored images over 10 different degradations for a different degree of channel misalignment and SNR.**

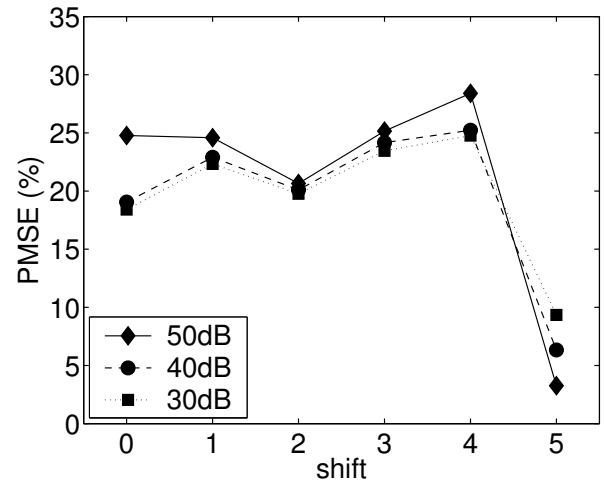


**Figure 6. AM-MAP algorithm performance on misaligned channels: Mean PMSE of restored images over 10 different degradations for a different degree of channel misalignment and SNR.**

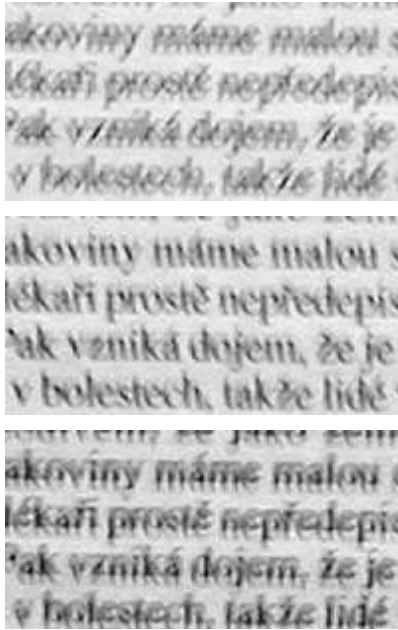


**Figure 7. Real data experiment: Three consecutive acquisitions of a text label attached to a vibrating machine. The images are cropped to  $100 \times 200$  size. Shift blurs and spatial misalignment of the images are clearly visible.**

and  $\|\mathbf{h}\|^2 = 0.25$ . The reconstructed label and the corresponding blur masks after 20 iterations are shown in Fig. 8. Observe that the restoration is slightly less successful at the image borders, especially close to the top edge, where only data from the third channel were available. We may conclude that the restoration was successful (the text is clearly readable) and that the spatial misalignment inherent to this type of problems poses no threat to proper functionality of the algorithm. Let us recall that no assumption about the shape of the blurring functions and no preprocessing of the input images were employed.

## 4 Conclusion

We have developed the iterative algorithm for MC blind deconvolution that searches for the MAP estimator. The prior density functions were derived from the variational integral defined on bounded variation functions and from the mutual relation of weakly coprime channels. The restoration is regularized with an anisotropic term for edge preservation and performs well on heavily degraded images with high SNR and shows better performance than the most recent multichannel method. We have also shown that the inaccurate registration of channels can be alleviated by prop-

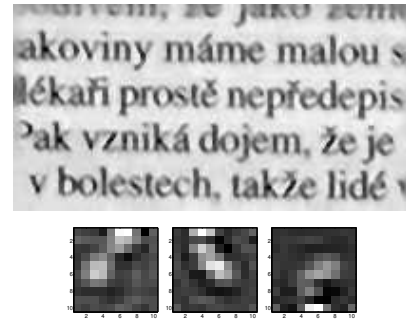


**Figure 8. Real data experiment: Reconstructed part of the label and the corresponding blurs (magnified) using the AM-MAP algorithm. The irregular vibration of the machine is well preserved in the blurs.**

erly overestimating the size of blurs. All previously published MC blind deconvolution methods assumed perfectly registered channels. To our knowledge, this is the only method dealing explicitly with misregistration of images in the multichannel framework and providing a successful solution to this problem.

## Acknowledgment

Financial support of this research was provided by the Grant Agency of the Czech Republic under the projects No. 102/00/1711 and 201/03/0675.

## References

- [1] A. Chambolle and P. Lions. Image recovery via total variation minimization and related problems. *Numer. Math.*, 76(2):167–188, Apr. 1997.
- [2] D. Geman and G. Reynolds. Constrained restoration and the recovery of discontinuities. *IEEE Trans. Pattern Anal.*, 14(3):367–383, Mar. 1992.
- [3] G. Giannakis and R. Heath. Blind identification of multichannel FIR blurs and perfect image restoration. *IEEE Trans. Image Processing*, 9(11):1877–1896, Nov. 2000.
- [4] G. Harikumar and Y. Bresler. Exact image deconvolution from multiple FIR blurs. *IEEE Trans. Image Processing*, 8:846–862, June 1999.
- [5] G. Harikumar and Y. Bresler. Perfect blind restoration of images blurred by multiple filters: Theory and efficient algorithms. *IEEE Trans. Image Processing*, 8(2):202–219, Feb. 1999.
- [6] H.-T. Pai and A. Bovik. Exact multichannel blind image restoration. *IEEE Signal Processing Letters*, 4(8):217–220, Aug. 1997.
- [7] H.-T. Pai and A. Bovik. On eigenstructure-based direct multichannel blind image restoration. *IEEE Trans. Image Processing*, 10(10):1434–1446, Oct. 2001.